Paramagnetism and macroscopic magnetic properties of single-crystal $Y_xGd_{1-x}Ba_2Cu_{2.43}Al_{0.19}O_{6+y}$

M. J. Qin, H. L. Ji, X. Jin, and X. X. Yao
Department of Physics and National Laboratory of Solid State Microstructures, Nanjing University, Nanjing 210008, People's Republic of China

X. S. Rong and Y. M. Ni
National Key Laboratory for Superconductivity, Institute of Physics, Chinese Academy of Sciences, Beijing 100080, People's Republic of China

L. Xiao and X. K. Fu
Beijing General Institute for Non-ferrous Metals, Beijing 100088, People's Republic of China
(Received 17 January 1994)

Magnetic measurements are carried out on single-crystal $Y_xGd_{1-x}Ba_2Cu_{2.43}Al_{0.19}O_{6+y}$ ($x=0,0.5$) samples. The magnetic-field dependence of the averaged paramagnetic moments carried by the rare-earth Gd^{3+} ions in these samples is well described by the extended Brillouin function. This paramagnetism tilts the magnetic hysteresis loop and broadens the widths of the magnetic hysteresis ΔM; therefore the magnetization critical-current density J_c based on the Bean critical-state model deviates from the intrinsic value. At temperature $T=4.2$ K, this deviation is up to 9% for the single-crystal $GdBa_2Cu_{2.43}Al_{0.19}O_{6+y}$ sample. At the end, the influence of the paramagnetism of Gd^{3+} ions on some other macroscopic magnetic properties is discussed.

I. INTRODUCTION

The study of high-temperature superconductivity in the $YBa_2Cu_3O_{7-\delta}$ (YBCO) systems is the most extensive of all the systems because of the high quality of YBCO single crystals prepared up to date. There have also been a lot of comparative investigations of YBCO and other systems with Y substituted by other rare-earth elements such as Nd, Sm, Eu, Gd, Dy, Ho, Er, Tm, Yb, and Lu.[1] The orthorhombic phases of these superconductors (denoted as *YR*BCO) all have a T_c as high as 90 K. Since most of the rare-earth ions carry large magnetic moments, many works have been devoted to the relationship between the magnetic ordering and superconductivity.[2,3]

It is shown in this paper that the paramagnetism of magnetic rare-earth Gd^{3+} ions broadens the apparent magnetic hysteresis loops of single-crystal $GdBa_2Cu_{2.43}Al_{0.19}O_{6+y}$ (denoted as GBCO) and $Y_{0.5}Gd_{0.5}Ba_2Cu_{2.42}Al_{0.19}O_{6+y}$ (denoted as YGBCO) superconductors; therefore, the derived magnetization critical-current density contains a systematic error, which is up to 9% for the single-crystal GBCO sample at temperature $T=4.2$ K. However, this effect has not been taken into account before to our knowledge.[4,5] Furthermore, the error caused by paramagnetism decreases with increasing temperature, and so it will modify the temperature dependence of the critical-current density J_c. From this point of view, the irreversibility line determined by the merging point of magnetic hysteresis loops or by that of field-cooled (FC) and zero-field-cooled (ZFC) susceptibility lines in dc magnetometry should also be corrected.

II. EXPERIMENTAL DETAILS

All experiments reported here have been performed on single-crystal GBCO and YGBCO ($Y_xGd_{1-x}Ba_2Cu_{2.43}Al_{0.19}O_{6+y}$ with $x=0$ and 0.5, respectively) samples. The synthesis and characterization of the samples have been reported elsewhere.[6] Briefly described, the single crystals were grown by the self-flux method. Single-crystal GBCO was grown with a starting composition of [Gd]: [Ba]: [Cu] = 1:4:10. High-purity (99.99%) or chemical reagent grade (99.9%) Gd_2O_3, $BaCO_3$, and CuO powders were weighed and well mixed, and the mixture was then put in an aluminum crucible of high purity and heat treated in air. The mixture was kept at 1050 °C for 1 h, and was slowly cooled to 850 °C with the cooling rate of 0.2 °C/h, then quickly cooled to room temperature.

In order to grow single-crystal YGBCO, we started with a 0.5:0.5:4:10 stoichiometry of [Y]: [Gd]: [Ba]: [Cu], and the soaking temperature was kept at 1040 °C for 1 h. Platelets of dimension 1–3 mm were found in the lower part of the melt. X-ray energy-dispersive spectrum (EDS) analyses using Noran series 2 (namely TN5502) on a 20-keV AMRAY 1840 scanning electron microscope showed that the cation composition in the platelets was [Y]: [Gd]: [Ba]: [Cu]: [Al] = 0.5:0.5:1.92:2.43:0.19. X-ray powder diffraction patterns of postannealed $Y_{0.5}Gd_{0.5}Ba_{1.93}Cu_{2.43}Al_{0.19}O_{6+y}$ contain all the peaks of the YBCO 123 orthorhombic phase, and no obvious peaks of impurity phases are observed. By these two measurements together with Laue backscattering diffraction patterns,[6] these platelets were confirmed to

be single crystal. Contamination of aluminum from the crucible is unavoidable; however, its influence on T_c is trivial, which may be explained by the accommodation of Al into the copper chains.

The as-grown single crystals were postannealed in pure oxygen at a pressure of 140–160 bar for 4–8 days. Such a high pressure greatly increases the diffusion constant of oxygen and shortens the annealing time. The single-crystal YGBCO and GBCO samples used in this work have T_c (onset) of 90 and 85 K by ac susceptibility measurement, and dimensions of $1.26\times1.28\times0.40$ mm^3 and $1.25\times1.60\times0.39$ mm^3, respectively.

Magnetic measurements were performed at two field orientations (along the c axis and the ab planes) on a commercial 8-T vibrating-sample magnetometer (Oxford Ltd., model 3001). The sample was first cooled from above T_c to the required temperature T in zero applied field. Then the applied field was swept at a rate of 12 mT s^{-1} to form the magnetic hysteresis loop. The magnetization relaxation measurement was performed at 4.2 K and 1 T with the zero-field-cooled process; the first point was recorded after a time delay of 80 s.

III. EFFECT OF THE PRAMAGNETISM

In Fig. 1 is the magnetization hysteresis loop of single-crystal GBCO ($H\|ab$) at $T=4.2$ K. As the field is increased within 3.1 kOe, the magnetization stays negative, as it must be in the case of ordinary superconductors containing no rare-earth ions. But in fields over 3.1 kOe the magnetization becomes positive and it shows a trend to saturation as the field is further increased. In this case, the sample continues to be in a superconducting state which is indicated by a magnetization hysteresis loop. The magnetization hysteresis loops of the GBCO sample ($H\|c$) and YGBCO sample ($H\|ab$) are shown in Figs. 2 and 3, respectively. The same hysteresis behavior shown in Figs. 1 is also observed, which can be attributed to the localized magnetic moments carried by the rare-earth Gd^{3+} ions in these samples. Ordering of the magnetic moments of Gd^{3+} in $Y_xGd_{1-x}Ba_2Cu_3O_{6+y}$, usually antiferromagnetically, takes place at extremely low temperature, which is about 2.2–2.6 K.[1] Above this temperature paramagnetism is exhibited. Therefore, above the magnetic ordering temperature of a $Y_xGd_{1-x}Ba_2Cu_3O_{6+y}$ sample, the experimentally measured magnetization contains two components: irreversible superconducting magnetization $M_{\rm sup}$ and the paramagnetic contribution $M_{\rm para}$,

$$M=M_{\rm sup}+M_{\rm para}\ ,$$

where, for simplicity, the reversible superconducting magnetization is neglected for its trivial influence on the results. The paramagnetic magnetization $M_{\rm para}$ increases with increasing field; therefore the experimentally measured magnetization M will become positive when $M_{\rm para}$ is larger than the increasing-field branch of the superconducting magnetization $M_{\rm sup}^{-}$. As the field becomes large enough, $M_{\rm para}$ will saturate, which results in the magnetization hysteresis loops shown in Figs. 1–3.

The magnetic-field dependence of the averaged paramagnetic magnetization,

$$M_{\rm para}=\frac{M^{+}+M^{-}}{2} \tag{1}$$

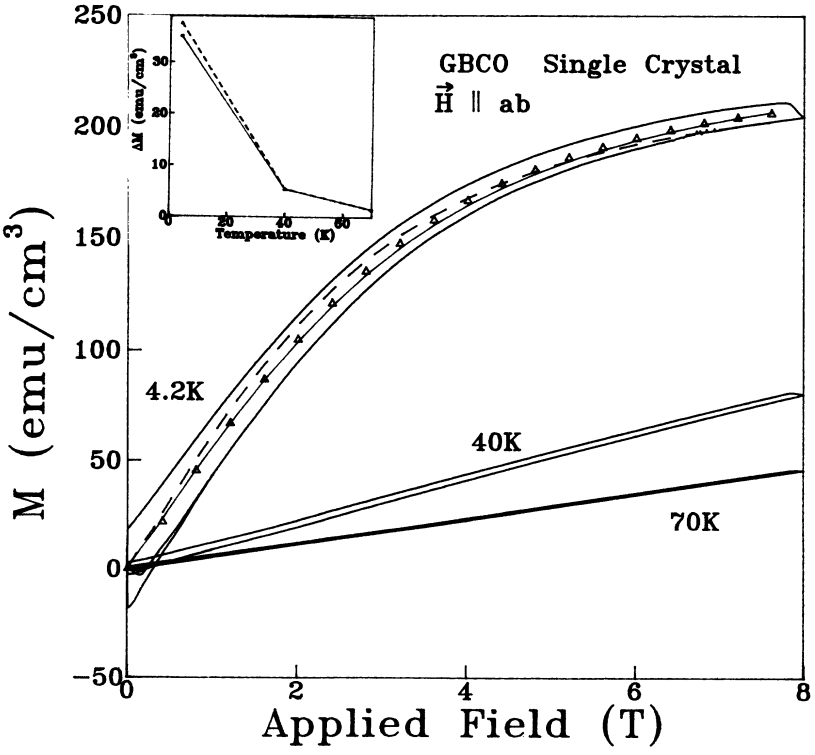

FIG. 1. Magnetization hysteresis loops of the single-crystal GBCO sample at the temperatures indicated and with the magnetic field $H\|ab$. Triangles represent $M_{\rm para}$, and solid and dashed lines are fits with Eq. (2) in which $x\propto1/(T+\theta_N)$ and $x\propto1/T$, respectively. Inset is the temperature dependence of ΔM before (dashed line) and after correction (solid line) for the paramagnetism of Gd^{3+} ions. (Solid and dashed lines in the inset are only guides for the eyes.)

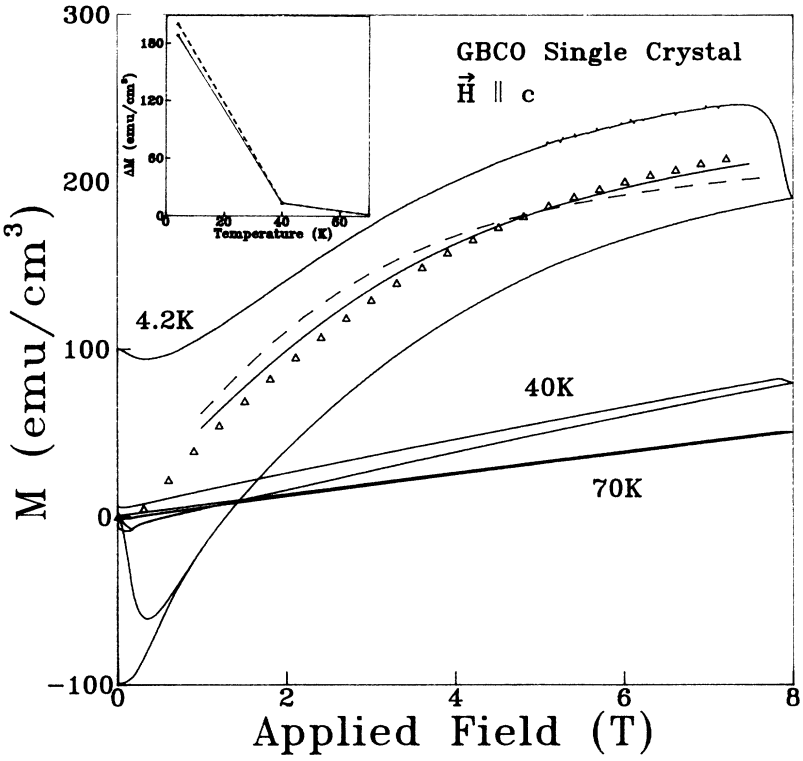

FIG. 2. Magnetization hysteresis loops of the single-crystal GBCO sample at the temperatures indicated and with the magnetic field $H\|c$. Triangles represent M_{para}, and solid and dashed lines are fits with Eq. (2) in which $x \propto 1/(T+\theta_N)$ and $x \propto 1/T$, respectively. Inset is the temperature dependence of ΔM before (dashed line) and after correction (solid line) for the paramagnetism of Gd^{3+} ions. (Solid and dashed lines in the inset are only guides for the eyes.)

(shown as triangles in Figs. 1–3), however, is not well described by a Brillouin function, as shown in Fig. 4 of Ref. 8 with $J=\frac{7}{2}$ which corresponds to the full moment of the free Gd^{3+} ion (dashed lines in Figs. 1–3). Therefore, it should take into account the antiferromagnetic interactions of the Gd^{3+} ions in low temperature. For the sake of simplicity, we extend the Brillouin function, which is the assumption of free Gd^{3+} ions to describe the magnetic-field dependence of M_{para}, rather than considering the molecular-field theory of antiferromagnetism.

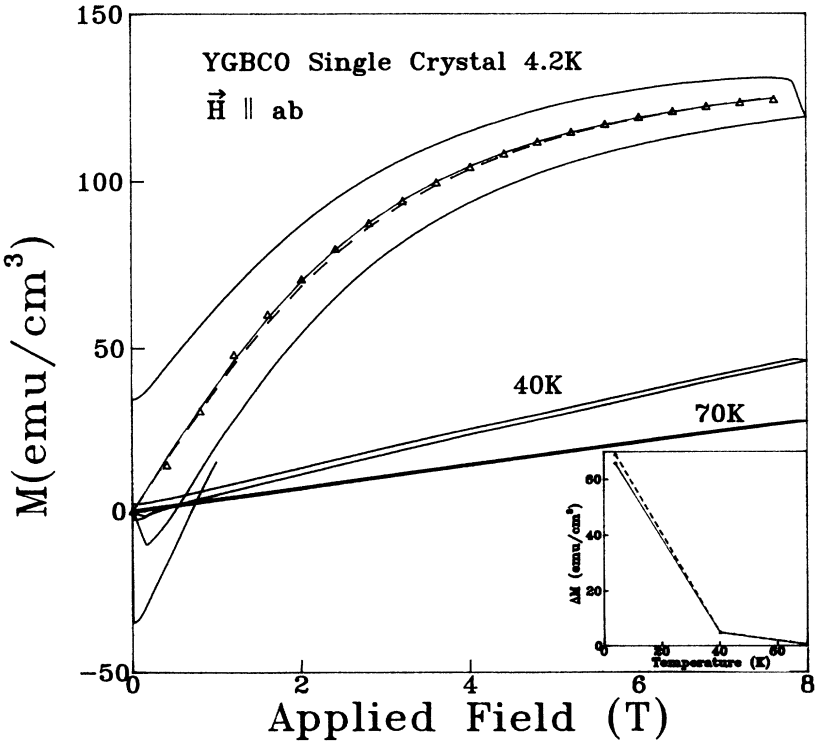

FIG. 3. Magnetization hysteresis loops of the single-crystal YGBCO sample at the temperatures indicated and with the magnetic field $H\|ab$. Triangles represent M_{para}, and solid and dashed lines are fits with Eq. (2) in which $x \propto 1/(T+\theta_N)$ and $x \propto 1/T$, respectively. Inset is the temperature dependence of ΔM before (dashed line) and after the correction (solid line) for the paramagnetism of Gd^{3+} ions. (Solid and dashed lines in the inset are only guides for the eyes.)

$$M_{\text{para}}=\frac{Jg\mu_B}{V}B_J(x)\ , \tag{2}$$

where μ_B is the Bohr magneton, g is the Landé factor of the Gd^{3+} ions, and V is the unit-cell volume of the YGBCO sample. $B_J(x)$ is the Brillouin function defined as

$$B_J(x)=\frac{1}{J}\left[\left(J+\tfrac{1}{2}\right)\coth\left(J+\tfrac{1}{2}\right)x-\tfrac{1}{2}\coth\frac{x}{2}\right]\ ,$$

where x is proportional to $1/(T+\theta_N)$ rather than $1/T$,

$$x=\frac{g\mu_B B}{k_B(T+\theta_N)}$$

where k_B is the Boltzmann constant, B is the flux density, T is the temperature, and θ_N is larger than the ordering temperature T_N.

We fit Eq. (2) to the experimental M_{para} vs H by treating θ_N as a fitting parameter. The results are shown as solid lines in Figs. 1–3, which are much better than the fits with the simple Brillouin function shown as dashed lines in these figures for comparison. The values of θ_N are 4.0, 5.2, and 2.5 in Figs. 1, 2, and 3, respectively. In all cases, values of the Landé factor g are taken to be 1.99, which is the Landé factor for the free Gd^{3+} ion.

In the limit of $x \ll 1$, namely, high temperature and low magnetic field, the limiting behavior of the Brillouin function is

$$B_J(x)=\frac{(J+1)x}{3}\ .$$

Substituting $B_J(x)$ in Eq. (2), we have the linear approximation $M_{\text{para}}=\chi B$, where χ is the volume susceptibility,

$$\chi=\frac{J(J+1)(g\mu_B)^2}{3k_B V(T+\theta_N)}\ . \tag{3}$$

As can be seen from Figs. 1–3, the paramagnetism of the Gd^{3+} ions tilts the magnetization hysteresis loop, and therefore the width of the magnetization hysteresis loop ΔM is broadened. We now consider a fully penetrated infinitely long slab of thickness d in a parallel field in the framework of the simple Bean critical-state model. Because the distribution of flux density in the slab during the increasing and decreasing-field processes at the same applied field is quite different, the averaged paramagnetic contribution should be different too; in the limit of $x \ll 1$, $M_{\text{para}}=\chi B$, its spatial average leads to the following expressions for the magnetization in the increasing- (M^-) and decreasing- (M^+) field branches:

$$M^+=\frac{\Delta M_{\text{sup}}}{2}+\chi\left[H_a+4\pi\frac{\Delta M_{\text{sup}}}{2}\right]$$

and

$$M^-=-\frac{\Delta M_{\text{sup}}}{2}+\chi\left[H_a-4\pi\frac{\Delta M_{\text{sup}}}{2}\right]$$

where ΔM_{sup} is the magnetic hysteresis if there is no paramagnetic contribution. Therefore

$$\Delta M=M^+-M^-=(1+4\pi\chi)\Delta M_{\text{sup}}\ ,$$

where ΔM is the apparent width of the magnetization hysteresis loop. It can be seen clearly that the width of magnetic hysteresis is broadened to an extent determined directly by the magnitude of χ. According to the Bean model, the width of the magnetic hysteresis is proportional to the critical-current density J_c, and therefore

$$J_c=\frac{J_c^A}{1+4\pi\chi}\ , \tag{4}$$

where J_c^A is the critical-current density calculated from the apparent magnetic hysteresis and J_c is the intrinsic critical-current density of the superconductor.

With θ_N derived from fitting Eq. (2) to the experimental data, χ is calculated with Eq. (3). Therefore, the intrinsic critical-current densities are obtained from Eq. (4), and are $J_c=0.91J_c^A$ and $J_c=0.92J_c^A$ at $T=4.2$ K, $H=0$ T for the GBCO sample with $H\|ab$ and $H\|c$, respectively, and $J_c=0.94J_c^A$ for the YGBCO sample. Because χ is proportional to $1/(T+\theta_N)$, as the temperature is increased, χ decreases quickly. For example, at $T=40$ K, $J_c=0.99J_c^A$ for the GBCO sample ($H\|ab$); therefore, the temperature dependence of the critical-current density should be modified, and the J_c-T curve should be flattened after this correction, which is shown clearly in the insets of Figs. 1–3.

IV. DISCUSSION

The above results are obtained based on single-crystal samples; however $GdBa_2Cu_3O_{6+y}$ sample prepared by melt-textured growth[7] (MTG) also shows the same behavior, which indicates the same role of Gd^{3+} ions in all YGBCO systems. The results are presented in Fig. 4 for comparison. $GdBa_2Cu_3O_{6+y}$ powders prepared by solid-state reaction were cold-pressed into a bar, sintered in air at 950 °C for 24 h, then put into a temperature-gradient furnace preheated to 1140 °C, and maintained for 10 min, and then quickly cooled to 1070 °C. After cooling to 970 °C at a rate of 1.5 °C/h, the samples were kept at the temperature for 3 h and finally cooled to room temperature. Postannealing of the as-grown sample was in flowing oxygen at 500 °C for about 100 h. The sample used in this work had a T_c (onset) of 93 K and ΔT_c of 0.6 K by ac susceptibility measurements, and dimensions of $1.75\times1.80\times0.23$ mm^3.

Shown in Fig. 5 is the magnetization hysteresis loop of the single-crystal YGBCO sample with $H\|c$, where the paramagnetism has less effect on the results. Therefore our discussions are mainly applicable to the direction with $H\|ab$, for which three factors may be responsible. First, the method used to derive the averaged paramagnetic magnetization M_{para} from Eq. (1) is satisfactory only in the case of the Bean model; however, when $H\|c$, the Bean model is a poor approximation, because ΔM decreases with the applied field up to 8 T. Second, in this field direction, M_{sup} is much larger than M_{para} (ΔM is one order of magnitude larger than that with $H\|ab$) which also makes it unsatisfactory to derive M_{para} from Eq. (1). The last factor is the large demagnetization fac-

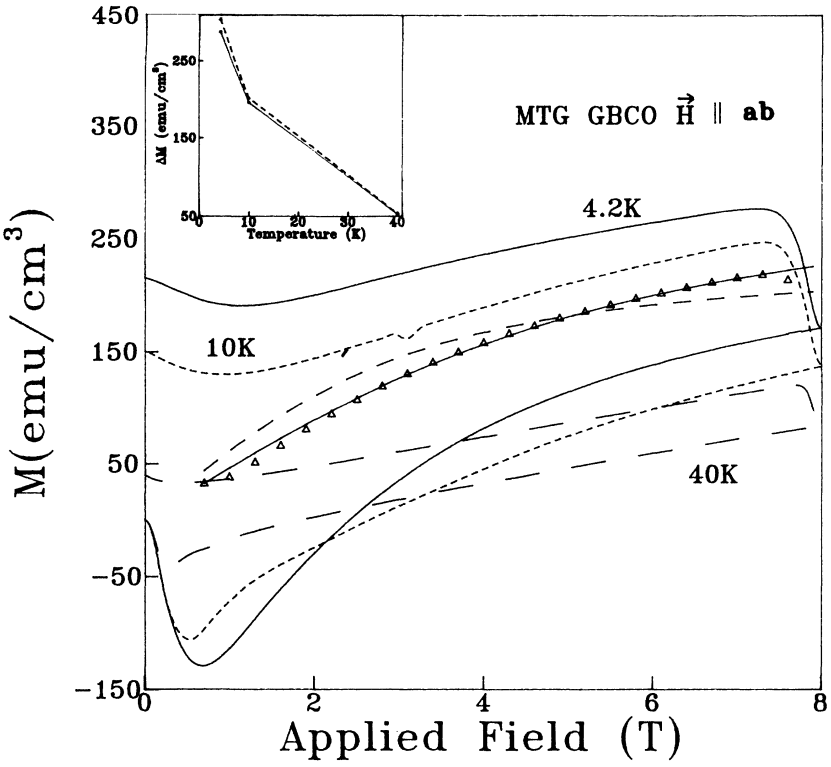

FIG. 4. Magnetization hysteresis loops of the melted GBCO sample at the temperatures indicated and with the magnetic field $H\|ab$. Triangles represent M_{para}, and solid and dashed lines are fits with Eq. (2) in which $x \propto 1/(T+\theta_N)$ and $x \propto 1/T$, respectively. Inset is the temperature dependence of ΔM before (dashed line) and after (solid line) correction for the paramagnetism of Gd^{3+} ions. (Solid and dashed lines in the inset are only guides for the eyes.)

tor along this field direction ($H\|c$) which makes it complicated to discuss the effect of paramagnetism.

The magnetization relaxation of the single-crystal GBCO sample at 4.2 K and 1 T is shown in Fig. 6. It is of interest to note that, unlike ordinary superconductors whose magnetization decreases with time towards an equilibrium value of about zero, the magnetization of the single-crystal GBCO sample increases with time towards a non-zero equilibrium value, which directly shows the contributions of the paramagnetism to the magnetization of the single-crystal GBCO sample.

The absolute magnetization relaxation rate $s=-\partial M_{\text{irr}}/\partial \ln t$ is also increased by a factor of $4\pi\chi$ for the paramagnetism; nevertheless the relative relaxation rate remains the same in the first-order approximation, and the derived U_0 is the same whether the effect described above is neglected or not. Similarly, when $\partial M_{\text{irr}}/\partial \ln t$ in the ZFC process is used to measure the penetration field of a superconductor,[9] the same enhancement factor of $4\pi\chi$ by Gd ions has no influence.

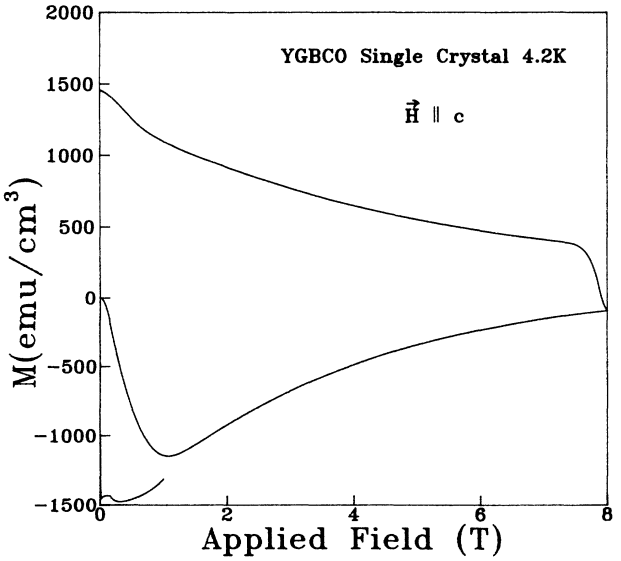

FIG. 5. Magnetization hysteresis loop of the single-crystal YGBCO sample at 4.2 K and with the magnetic field $H\|c$.

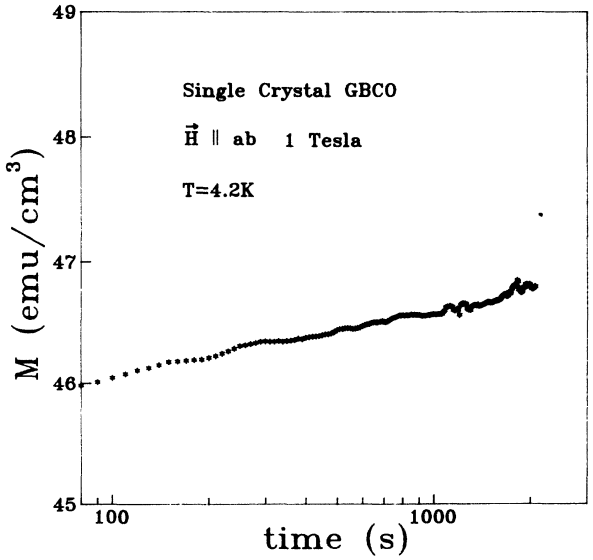

FIG. 6. Magnetization relaxation at a given field $H=1$ T for the single-crystal GBCO sample at 4.2 K.

V. CONCLUSION

In summary, we have shown that, above the magnetic ordering temperature T_N, the magnetic-field dependence of the paramagnetic magnetization carried by Gd^{3+} ions in YGBCO systems is well described by the extended Brillouin function. We have also shown the enhancement effect of magnetic hysteresis loops by the paramagnetism of Gd^{3+} in these systems, which is evident at low temperature. This effect exhibits itself in the measurements of critical-current density, absolute magnetization relaxation rate, irreversibility line, and the effective activation energy. In the comparative study of the magnetic properties of superconductors substituted by rare-earth elements of a variety of concentrations, this correction is essential.

[1]J. T. Market, U. Dalichaouch, and M. B. Maple, in *Physical Properties of High Temperature Superconductors I,* edited by D. M. Ginsberg (World Scientific, Singapore, 1989), p. 265, and the references therein.

[2]M. Furayama, I. Iguchi, and U. Muto, Physica B **165&166**, 1191 (1990).

[3]D. W. Murphy, S. A. Sunshine, P. K. Gallagher, R. B. van Dover, R. J. Cava, B. Batlogg, S. M. Zahuarak, and L. F. Schneemeyer, Phys. Rev. Lett. **58**, 1888 (1987).

[4]L. F. Schneemeyer, E. M. Gyorgy, and J. V. Waszczak, Phys. Rev. B **36**, 8804 (1987).

[5]S. K. Malik, R. Prasad, N. C. Soni, C. V. Tomy, D. T. Adroja, A. Mohan, C. K. Gupta, S. G. Sankar, Y. Xu, E. B. Boltich, R. T. Obermyer, L. N. Yannopoulos, and W. E. Wallace, J. Magn. Magn. Mater. **72**, L4 (1988).

[6]H. L. Ji, C. G. Zhang, X. Jin, J. B. Ji, X. N. Xu, R. X. Lu, X. X. Yao, and G. D. Sheng, Supercond. Sci. Technol. **5**, 609 (1992).

[7]H. T. Ren, Q. He, L. Xiao, R. W. Wang, D. G. Yu, C. G. Cui, and S. L. Li, Cryogenics **30**, S837 (1990).

[8]*High Temperature Superconductivity from Russia,* edited by A. I. Larkin and N. V. Zavaritsky (World Scientific, Singapore, 1989), p. 152.

[9]D. Shi and S. Salem-Sugui, Jr., Phys. Rev. B **44**, 7647 (1991).